Calculation of the micromaser spectrum. II. Eigenvalue approach

K. Vogel and W. P. Schleich*
Abteilung für Quantenphysik, Universität Ulm, W-7900 Ulm, Germany

M. O. Scully*
Department of Physics, Texas A&M University, College Station, Texas 77843

H. Walther
Max-Planck-Institut für Quantenoptik, W-8046 Garching, Germany
(Received 10 February 1993)

We calculate the micromaser spectrum via the eigenvalues and eigenvectors of the master equation. We show that (i) it is not always the lowest eigenvalue which governs the linewidth and (ii) the oscillations in the linewidth originate from an interplay between *two* eigenvalues.

PACS number(s): 42.50.Dv, 42.52+x, 32.80.-t

I. INTRODUCTION

In the first [1] of these two papers on the micromaser spectrum (hereafter referred to as paper I) we have presented a Green's-function approach as well as various approximate analytical expressions for the micromaser linewidth [2]. In the present paper we pursue another approach: We obtain the spectrum numerically via the eigenvalues and the eigenvectors of the micromaser master equation. We identify the contributions of the individual eigenvalues to the spectrum and show that the micromaser linewidth is not necessarily determined by the lowest eigenvalue. Moreover, in the neighborhood of trapping states *two* eigenvalues have an essential influence on the linewidth.

The paper is organized as follows: In Sec. II we express the correlation function $K(t) = \langle a^\dagger(t)a(0)\rangle$ governing the spectrum in terms of the off-diagonal elements $\tilde{\rho}_{n,n+1} = \tilde{\rho}_n^{(1)}$ of the "moment" operator $\tilde{\rho}$ which satisfies the equation of motion for the density operator ρ_f of the maser field *subject* to the initial condition $\tilde{\rho}_n^{(1)} = \sqrt{n+1}\,P_{n+1}$. Here P_n is the steady-state photon statistics. We therefore cast in Sec. III the equation of motion for the maser density operator ρ_f, which is identical to that for $\tilde{\rho}$, into a system of linear differential equations. This allows us to express the quantities of interest such as $K(t)$ by the appropriate superposition of eigenvectors of the corresponding matrix. In particular, the spectrum of the maser is the sum of Lorentzian distributions, each of which has a width given by the real part of an eigenvalue. The weight of each Lorentzian distribution follows from the initial condition for $\tilde{\rho}_n^{(1)}$. We determine the eigenvalues and eigenvectors numerically in Sec. IV and discuss their behavior as a function of the pump parameter and the number of thermal photons. We conclude by summarizing our main results in Sec. V.

II. SPECTRUM FROM THE DECAY OF OFF-DIAGONAL ELEMENTS OF THE DENSITY MATRIX

In the present section we relate the time dependence of the two-time correlation function

$$K(t) = \langle a^\dagger(t)a(0)\rangle \tag{2.1}$$

to the time dependence of the off-diagonal elements of the field density operator. As in paper I we define the micromaser spectrum as the Fourier transform

$$S(\omega-\omega_c) = \mathrm{Re}\int_0^\infty K(t)\,e^{-i(\omega-\omega_c)t}\,dt \tag{2.2}$$

of the two-time correlation function $K(t)$. Here ω_c denotes the frequency of the cavity field.

The central problem of the calculation of the micromaser spectrum is therefore to find the time dependence of $K(t)$. With the help of the time evolution operator $U(t)$ for the combined field (f) – reservoir (r) system the correlation function $K(t)$ reads [3]

$$K(t) = \mathrm{Tr}_{f,r}\left[U^\dagger(t)a^\dagger(0)U(t)a(0)\rho_{f,r}(0)\right] \tag{2.3}$$

or

$$K(t) = \mathrm{Tr}_f\left[a^\dagger(0)\tilde{\rho}(t)\right], \tag{2.4}$$

where we have defined the trace over the reservoir of the first moment of the field operator as

$$\tilde{\rho}(t) \equiv \mathrm{Tr}_r\left[U(t)a(0)\rho_{f,r}(0)U^\dagger(t)\right]. \tag{2.5}$$

We therefore call $\tilde{\rho}$ the moment operator. In the Markov approximation the operator $\tilde{\rho}(t)$ satisfies [4] the equation of motion for the field density operator

$$\rho_f(t) \equiv \mathrm{Tr}_r \left[U(t)\rho_{f,r}(0)U^\dagger(t)\right] \tag{2.6}$$

with the initial condition

$$\tilde{\rho}(0) = a(0)\rho_f(0)\,. \tag{2.7}$$

Since we are only interested in the correlation function $K(t)$ at steady-state we choose the steady-state solution of the field density operator $\rho_f^{(s)}$ as the initial condition, that is,

$$\tilde{\rho}(0) = a(0)\rho_f^{(s)}\,. \tag{2.8}$$

In the number state representation we can perform the trace in Eq. (2.4) and find

$$\begin{aligned} K(t) &= \sum_{n=0}^{\infty} \langle n|a^\dagger(0)\tilde{\rho}(t)|n\rangle \\ &= \sum_{n=0}^{\infty} \sqrt{n+1}\,\langle n|\tilde{\rho}(t)|n+1\rangle \end{aligned} \tag{2.9}$$

or

$$K(t) = \sum_{n=0}^{\infty} \sqrt{n+1}\,\tilde{\rho}_{n,n+1}(t)\,. \tag{2.10}$$

The initial condition Eq. (2.8) reads

$$\begin{aligned} \tilde{\rho}_{n,n+1}(0) &= \langle n|a(0)\rho_f^{(s)}|n+1\rangle \\ &= \sqrt{n+1}\,\langle n+1|\rho_f^{(s)}|n+1\rangle \end{aligned} \tag{2.11}$$

or

$$\tilde{\rho}_{n,n+1}(0) = \sqrt{n+1}\,P_{n+1}\,, \tag{2.12}$$

where $P_n = \langle n|\rho_f^{(s)}|n\rangle$ denotes the steady-state photon statistics.

III. SOLUTION OF MASTER EQUATION IN TERMS OF EIGENVALUES AND EIGENVECTORS

So far our considerations are rather general; we now concentrate on the micromaser. In the previous section we have shown that the moment operator $\tilde{\rho}$ which determines the time dependence of $K(t)$ satisfies the master equation for the micromaser field. The equation of motion for the density matrix elements

$$\rho_{n,n+k} \equiv \langle n|\rho_f|n+k\rangle \equiv \rho_n^{(k)} \tag{3.1}$$

of the micromaser field in the interaction picture reads [5]

$$\dot{\rho}_n^{(k)}(t) = \mathcal{A}_n^{(k)}\,\rho_{n-1}^{(k)} + \mathcal{B}_n^{(k)}\,\rho_n^{(k)} + \mathcal{C}_n^{(k)}\,\rho_{n+1}^{(k)}\,, \tag{3.2}$$

where $\mathcal{C}_n^{(k)}$, $\mathcal{B}_n^{(k)}$, and $\mathcal{A}_n^{(k)}$ are given by

$$\mathcal{A}_n^{(k)} = r\sin\left(g\tau\sqrt{n}\right)\sin\left(g\tau\sqrt{n+k}\right) + \gamma n_b\sqrt{n\,(n+k)}\,, \tag{3.3a}$$

$$\begin{aligned} \mathcal{B}_n^{(k)} = &-r\left[1-\cos\left(g\tau\sqrt{n+1}\right)\cos\left(g\tau\sqrt{n+1+k}\right)\right] \\ &-\gamma\,(n_b+1)\left(n+\frac{k}{2}\right) - \gamma n_b\left(n+1+\frac{k}{2}\right)\,, \end{aligned} \tag{3.3b}$$

$$\mathcal{C}_n^{(k)} = \gamma\,(n_b+1)\sqrt{(n+1)\,(n+1+k)}\,. \tag{3.3c}$$

Here r is the injection rate of Rydberg atoms whose time of flight through and coupling strength with the cavity field are given by τ and g, respectively. The cavity decay rate is denoted by γ and n_b is the mean number of thermal photons.

For our numerical calculations we interpret the matrix elements $\tilde{\rho}_n^{(k)}(t) = \langle n|\tilde{\rho}(t)|n+k\rangle$ of the operator $\tilde{\rho}(t)$ as the nth component of the vector $\mathbf{x}^{(k)}(t)$, that is,

$$\left[\mathbf{x}^{(k)}\right]_n \equiv \tilde{\rho}_n^{(k)}\,. \tag{3.4}$$

When we recall that $\tilde{\rho}_n^{(k)}(t)$ satisfies Eq. (3.2) with $\tilde{\rho}_n^{(k)}(t)$ replacing $\rho_n^{(k)}(t)$, the equation of motion for the vector $\mathbf{x}^{(k)}(t)$ reads

$$\dot{\mathbf{x}}^{(k)} = \mathbf{Q}^{(k)}\mathbf{x}^{(k)}\,, \tag{3.5}$$

where $\mathbf{Q}^{(k)}$ is a tridiagonal matrix with the elements

$$Q_{n,n-1}^{(k)} = \mathcal{A}_n^{(k)}\,, \quad Q_{n,n}^{(k)} = \mathcal{B}_n^{(k)}\,, \quad Q_{n,n+1}^{(k)} = \mathcal{C}_n^{(k)}\,. \tag{3.6}$$

The time-dependent solution of Eq. (3.5) can be expanded according to

$$\mathbf{x}^{(k)}(t) = \sum_l c_l^{(k)}\,\mathbf{x}_l^{(k)}\,e^{-\lambda_l^{(k)}t}\,, \tag{3.7}$$

where $\mathbf{x}_l^{(k)}$ and $\lambda_l^{(k)}$ follow from the eigenvalue equation

$$\mathbf{Q}^{(k)}\mathbf{x}_l^{(k)} = -\lambda_l^{(k)}\mathbf{x}_l^{(k)}\,. \tag{3.8}$$

The coefficients $c_l^{(k)}$ have to be determined such that

$$\mathbf{x}^{(k)}(0) = \sum_l c_l^{(k)}\,\mathbf{x}_l^{(k)} \tag{3.9}$$

fulfills the initial condition

$$\begin{aligned} \left[\mathbf{x}^{(k)}(0)\right]_n \equiv \tilde{\rho}_n^{(k)}(0) &= \sqrt{n+1}\,\rho_{n+1,n+k}(0) \\ &= \sqrt{n+1}\,\rho_{n+1}^{(k-1)}(0)\,, \end{aligned} \tag{3.10}$$

which is the number state representation of Eq. (2.7).

According to Eq. (2.10) only $\tilde{\rho}_n^{(1)}(t)$ and therefore only $\mathbf{x}^{(1)}(t)$ has an influence on the micromaser spectrum. We therefore confine ourselves for the remainder of the paper to the case $k = 1$. Furthermore, we investigate the micromaser spectrum at steady state, where we have

$$\left[\mathbf{x}^{(1)}(0)\right]_n \equiv \tilde{\rho}_n^{(1)}(0) = \sqrt{n+1}\,P_{n+1}\,. \tag{3.11}$$

We obtain the steady-state photon statistics P_n from Eq. (3.2) using the condition of detailed balance and find [5,6]

$$P_n = P_0 \prod_{\nu=1}^{n} \left(\frac{n_b}{n_b+1} + \frac{N \sin^2(g\tau\sqrt{\nu})}{\nu(n_b+1)} \right) , \qquad (3.12)$$

where P_0 denotes a normalization constant and $N = r/\gamma$ represents the number of atoms passing through the cavity in a time γ^{-1}.

The coefficients $c_l^{(1)}$ can be determined numerically from Eq. (3.9) with $k = 1$, that is,

$$\sum_l c_l^{(1)} \mathbf{x}_l^{(1)} = \mathbf{x}^{(1)}(0) \qquad (3.13)$$

together with Eqs. (3.11) and (3.12). Equation (3.13) is the expansion of the vector $\mathbf{x}^{(1)}(0)$ of the initial condition, Eq. (3.11), in eigenvectors. We determine [7] the coefficients $c_l^{(1)}$ by noting that the eigenvalues $\bar{\lambda}_l^{(1)}$ and the eigenvectors $\mathbf{y}_l^{(1)}$ of the transposed matrix $\left[\mathbf{Q}^{(1)}\right]^T$ are related to the eigenvalues $\lambda_l^{(1)}$ and eigenvectors $\mathbf{x}_l^{(1)}$ of the matrix $\mathbf{Q}^{(1)}$ via

$$\bar{\lambda}_l^{(1)} = \lambda_l^{(1)} , \qquad \left[\mathbf{y}_{l_1}^{(1)}\right]^T \mathbf{x}_{l_2}^{(1)} = \delta_{l_1 l_2} . \qquad (3.14)$$

When we multiply Eq. (3.13) by $\left[\mathbf{y}_l^{(1)}\right]^T$ and use the orthogonality relation, Eq. (3.14), the coefficients $c_l^{(1)}$ read

$$c_l^{(1)} = \left[\mathbf{y}_l^{(1)}\right]^T \mathbf{x}^{(1)}(0) . \qquad (3.15)$$

We have now all ingredients of the correlation function $K(t)$. Equation (3.4) expresses the correlation function $K(t)$, Eq. (2.10), as

$$K(t) = \sum_n \sqrt{n+1}\, \tilde{\rho}_n^{(1)}(t) = \sum_n \sqrt{n+1} \left[\mathbf{x}^{(1)}(t)\right]_n \qquad (3.16)$$

which with the help of Eq. (3.7) reads

$$K(t) = \sum_l K_l\, e^{-\lambda_l^{(1)} t} . \qquad (3.17)$$

Here the contribution K_l of the lth eigenvalue to the correlation function follows from Eq. (3.15) and reads

$$K_l = \sum_m \left[\mathbf{y}_l^{(1)}\right]_m \sqrt{m+1}\, P_{m+1} \times \sum_n \sqrt{n+1} \left[\mathbf{x}_l^{(1)}\right]_n . \qquad (3.18)$$

Therefore we have to calculate the eigenvalues $\lambda_l^{(1)}$ as well as the right- and left-sided eigenvectors $\mathbf{x}_l^{(1)}$ and $\mathbf{y}_l^{(1)}$ of the matrix $\mathbf{Q}^{(1)}$, respectively. The Fourier transform of Eq. (3.17),

$$S(\omega - \omega_c) = \mathrm{Re} \sum_l \frac{K_l}{\lambda_l^{(1)} + i(\omega - \omega_c)} , \qquad (3.19)$$

is then the spectrum of the micromaser: It consists of Lorentzian distributions, weighted by K_l. The width of each individual Lorentzian distribution is the real part of the eigenvalue $\lambda_l^{(1)}$.

IV. DISCUSSION

We start our analysis by first discussing the eigenvalues of the micromaser master equation and then show how the micromaser spectrum emerges from these eigenvalues.

Since the matrix $\mathbf{Q}^{(1)}$ is not symmetric the eigenvalues can be complex. In Fig. 1 we show the real part and the imaginary part of the first 10 eigenvalues $\lambda_l^{(1)}$ of the matrix $\mathbf{Q}^{(1)}$ normalized to the cavity damping constant γ as a function of the pump parameter $\theta = \sqrt{N} g\tau$. Here we have chosen $N = 50$ and $n_b = 10^{-4}$. We have obtained this figure by numerically calculating the eigenvalues of the truncated matrix $\mathbf{Q}^{(1)}$ of size 100×100. For $\theta = 0$—the field in the resonator shows only decay—the eigenvalues take a simple analytic expression

$$\lambda_l^{(1)} = \left(l - \tfrac{1}{2}\right)\gamma , \quad l = 1, 2, 3, \ldots . \qquad (4.1)$$

For increasing pump parameter θ the eigenvalues decrease assuming a minimum around the first maser threshold, $\theta \approx 1$, and then rapidly increase. This behavior is analogous to that of the ordinary laser [8]. However, for larger pump parameters they cross each other and especially the higher eigenvalues create a rather complex picture. As an example we have plotted the neighborhood of $\theta = 2\pi$ where the real parts of two eigenvalues

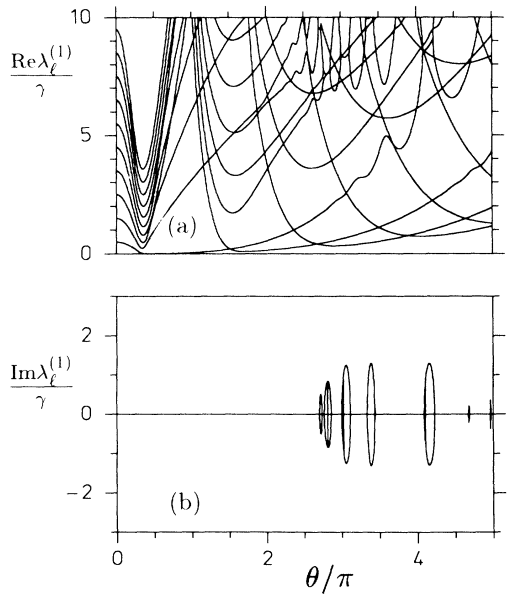

FIG. 1. The real part (a) and the imaginary part (b) of the 10 lowest eigenvalues $\lambda_l^{(1)}/\gamma$ of the micromaser master equation as a function of the pump parameter $\theta = \sqrt{N} g\tau$. The eigenvalues are normalized to the decay time γ^{-1} of the cavity. The scaled injection rate $N = r/\gamma$ of atoms has the value $N = 50$ and the number n_b of thermal photons is $n_b = 0.05$.

merge into one as shown in Fig. 2(a). This merging is accompanied by a bifurcation in the imaginary part displayed in Fig. 2(b). It is interesting to note that the eigenvalues of the Brownian motion in a periodic potential display a similar bifurcation behavior [9].

From this "chaotic" behavior of the eigenvalues it seems impossible to understand the micromaser linewidth [full width of the spectrum $S(\omega - \omega_c)$ at half maximum] shown in the top row of Fig. 3 for different numbers of thermal photons and calculated via the eigenvalue method. Only the combined knowledge of the eigenvalues along with the weight factors K_l gives insight into the behavior of the micromaser linewidth as a function of the pump parameter. For this purpose we show in the second row of Fig. 3 the first three eigenvalues along with the corresponding weight factors K_1, K_2, and K_3. Note that we do not number the eigenvalues according to their size but rather according to their natural dependence on θ. In this notation curve (1) corresponds to the first eigenvalue, curve (2) to the second, and curve (3) describes the third eigenvalue. The weight factors K_1, K_2, and K_3 correspond to these eigenvalues. This way of numbering brings out most clearly the influence of various eigenvalues via their factors K_l. The higher weight factors are negligible for the parameters discussed here and we therefore have suppressed them. To analyze the influence of the number of thermal photons n_b the left column discusses the case of $n_b = 10^{-4}$ whereas the right column contains $n_b = 0.05$. We are now able to explain how the weight factors K_l together with their corresponding eigenvalues produce the dependence of the linewidth on the pump parameter θ. We first consider the left column of Fig. 3 and start our discussion with values of $\theta < 1.5\pi$. We note that in this regime the weight factor K_1 is almost unity whereas K_2 and K_3 are almost zero. Hence a single eigenvalue, namely the first eigenvalue, governs the micromaser linewidth. Moreover it is the lowest eigenvalue. This is in complete agreement with ordinary laser theory. However, around $\theta = 1.5\pi$ the first eigenvalue crosses the second eigenvalue. Note that it is still the first eigenvalue ($K_1 = 1$) which governs the spectrum but now it is not the lowest one. In the neighborhood of $\theta = 2\pi$ an interesting interplay between the two eigenvalues begins. Here the spectrum consists of two Lorentzian distributions with different widths $\lambda_1^{(1)}$ and $\lambda_2^{(1)}$ and weight factors K_1 and K_2. These jumps between the two eigenvalues give rise to the narrow struc-

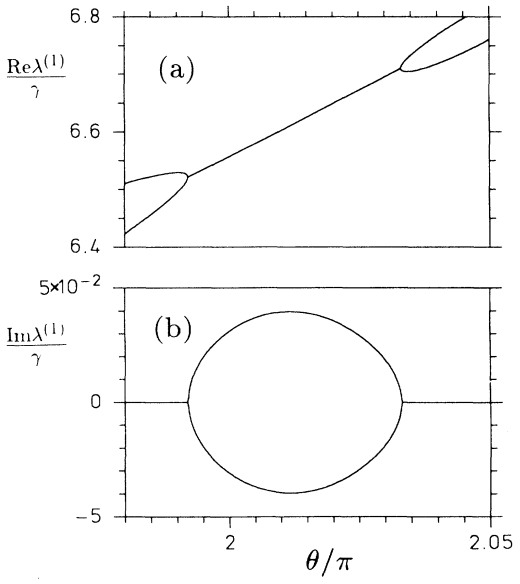

FIG. 2. When the real parts of two normalized eigenvalues $\lambda^{(1)}/\gamma$ of the micromaser master equation merge into one as shown in (a) they assume a nonvanishing imaginary part as indicated in (b). Here we have chosen $N = 50$ and $n_b = 10^{-4}$.

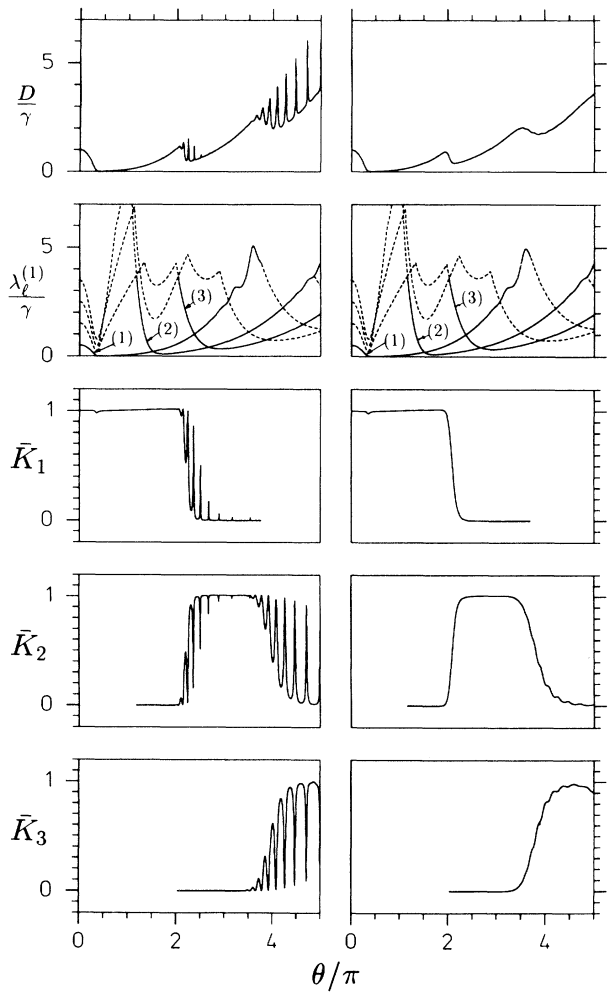

FIG. 3. The micromaser linewidth D/γ (top row), the three lowest eigenvalues $\lambda_1^{(1)}/\gamma$, $\lambda_2^{(1)}/\gamma$, and $\lambda_3^{(1)}/\gamma$ of the matrix $\mathbf{Q}^{(1)}$ and their normalized contributions $\bar{K}_1 = K_1/\sum_l K_l$, $\bar{K}_2 = K_2/\sum_l K_l$, and $\bar{K}_3 = K_3/\sum_l K_l$, to the correlation function $K(t) = \langle a^\dagger(t)a(0)\rangle$ as a function of the pump parameter θ. The solid lines in the row second from the top show the eigenvalues that essentially determine the micromaser spectrum. The left column is for $n_b = 10^{-4}$ whereas the right column is for $n_b = 0.05$. In both columns the scaled injection rate of the atoms is $N = 50$.

tures in the spectrum which are so intimately related [1,2] to trapping states. Note that in this regime the third eigenvalue crosses the other two but does not play any role yet ($K_3 \approx 0$). In particular, around $\theta = 3\pi$ the first two eigenvalues lie even higher than the third. In the vicinity of $\theta = 3.5\pi$, that is, the second group of trapping states, the first eigenvalue switches off completely and now an interplay between the second and the third eigenvalue starts.

The presence of thermal photons does not manifest itself in the eigenvalues as shown in the second row of Fig. 3. However, it smears out the narrow structures in K_1, K_2, and K_3, that is, the jumps between K_1 and K_2 and between K_2 and K_3. This gives rise to a sharp but smooth turnoff of the first eigenvalue around $\theta = 2\pi$ and switch on of $\lambda_2^{(1)}$. Similarly in the vicinity of $\theta \approx 3.7\pi$, the eigenvalues $\lambda_2^{(1)}$ gets switched off in favor of $\lambda_3^{(1)}$. Hence around these values of the pump parameter the linewidth makes a smooth transition from one eigenvalue to the next.

V. CONCLUSION

We conclude by summarizing our main results. We have analyzed the micromaser spectrum by numerically solving for the eigenvalues and the eigenvectors of the master equation for the micromaser. The spectrum consists of a sum of Lorentzian distributions—the width of each Lorentzian distribution is the real part of a single eigenvalue and its weight factor results from the expansion of the initial condition into eigenvectors. We have discussed the eigenvalues, which can assume imaginary parts, in their dependence on the pump parameter and the number of thermal photons. However, for the understanding of the spectrum for the parameter of interest discussed here the three lowest eigenvalues suffice. In particular, the present analysis summarized in Fig. 3 reveals three striking features: (i) The micromaser linewidth is *not* determined by the lowest eigenvalue. (ii) There exist regions of the pump parameter in which the linewidth is determined by a *single* eigenvalue. (iii) In the neighborhood of trapping states *two* eigenvalues have an essential influence on the linewidth. For low cavity temperatures the linewidth jumps between those eigenvalues whereas for higher cavity temperatures it changes smoothly from one eigenvalue to the other.

ACKNOWLEDGMENTS

The authors would like to thank R. J. Brecha, M. Fleischhauer, C. Keitel, L. Narducci, C. Su, and S. Y. Zhu for many valuable discussions. M.O.S. wishes to thank the ONR for support of his research.

* Also at Max-Planck-Institut für Quantenoptik, W-8046 Garching, Germany.

[1] Tran Quang, G. S. Agarwal, J. Bergou, M. O. Scully, H. Walther, W. P. Schleich, and K. Vogel, preceding paper, Phys. Rev. A **48**, 803 (1993).

[2] For a detailed balance approach towards the micromaser linewidth and a proposed measurement scheme using a Ramsey technique, see also M. O. Scully, H. Walther, G. S. Agarwal, Tran Quang, and W. Schleich, Phys. Rev. A **44**, 5992 (1991).

[3] M. O. Scully and W. E. Lamb, Jr., Phys. Rev. **159**, 208 (1967); see also M. Sargent, M. O. Scully, and W. E. Lamb, *Laser Physics* (Addison-Wesley, Reading, MA, 1974).

[4] C. W. Gardiner, *Handbook of Stochastic Methods* (Springer, Heidelberg, 1983).

[5] L. Lugiato, M. O. Scully, and H. Walther, Phys. Rev. A **36**, 740 (1987).

[6] P. Filipowicz, J. Javanainen, and P. Meystre, Phys. Rev. A **34**, 4547 (1986).

[7] Another way of finding the coefficients $c_i^{(1)}$ consists of solving the set of linear equations for $c_i^{(1)}$ defined by Eq. (3.13) for given $\mathbf{x}_i^{(1)}$ and $\mathbf{x}^{(1)}(0)$.

[8] H. Risken and H. D. Vollmer, Z. Phys. **201**, 323 (1967); H. Haken, *Handbuch der Physik* (Springer, Heidelberg, 1970), Vol. XXV/2c; Y. K. Wang and W. E. Lamb, Jr., Phys. Rev. A **8**, 866 (1973); K. Seybold and H. Risken, Z. Phys. **267** (1974); H. Risken, *The Fokker-Planck Equation* (Springer, Heidelberg, 1989), Chap. 12.

[9] H. D. Vollmer and H. Risken, Physica **110A**, 106 (1982); H. Risken, *The Fokker-Planck Equation* (Springer, Heidelberg, 1989), Chap. 11.